Resistive switching and optical properties of strontium ferrate titanate thin film prepared via chemical solution deposition

Jun Li (lijun19930818@163.com)
Guangdong University of Technology https://orcid.org/0000-0002-3039-1124
Xingui Tang
Guangdong University of Technology
Qiuxiang Liu
Guangdong University of Technology
Yanping Jiang
Guangdong University of Technology
Zhenxun Tang
Guangdong University of Technology

Research Article

Keywords: SrTiO3, thin films, resistive switching, oxygen vacancy, first principles

Posted Date: September 21st, 2020

DOI: https://doi.org/10.21203/rs.3.rs-80169/v1

Version of Record: A version of this preprint was published at Journal of Advanced Ceramics on September 20th, 2021. See the published version at https://doi.org/10.1007/s40145-021-0483-0.

Abstract

The polycrystalline strontium ferrate titanate ($SrFe_{0.1}Ti_{0.9}O_3$, abbreviated to SFTO) thin films have been successfully prepared by chemical solution method. By analyzing the current-voltage (I-V) characteristics, we discuss the conduction mechanism of SFTO. It is found that the number of oxygen vacancy defects is increased by Fe ions doping, making SFTO be with better resistive switching property. Fe ions doping can also enhance the absorption of strontium titanate to be exposed to visible light, which is associated with the change of energy band. The band gap width (2.84 eV) of SFTO films is figured out, which is less than that of pure strontium titanate. Due to more oxygen vacancy defects caused by Fe ions doping, the band gap width of strontium titanate was reduced slightly. The defect types of SFTO thin films can be determined by electron paramagnetic resonance spectroscopy. In addition, we analyzed the energy band and state density of SFTO by first-principle calculation based on density functional theory, and found that Fe ions doping can reduce the band gap width of strontium titanate with micro-regulation on the band structure. A chemical state of SFTO was analyzed by X-ray photo electron spectroscopy. At the same time, the structure and morphology of SFTO were characterized by X-ray diffraction and scanning electron microscope. This study deepened the understanding of the influence of Fe ions doping on the structure and properties of strontium ferrate titanate, which is expected to be a functional thin film material for memristor devices.

1. Introduction

During the past few decades, a large number of experimental and theoretical studies on ABO_3 perovskite compounds have been carried out, especially the typical material $SrTiO_3$. One motive force to study $SrTiO_3$ perovskite is the opportunity to regulate and control its electronic and ionic defect structures, so as to gain a wide range of applications (energy harvesting, memory device, oxygen sensor, catalysis, fuel cell cathodes, etc.) [1-5]. There are a number of researches by first-principles studies of defective perovskite to investigate electronic structure and performance [6-11]. As for $SrTiO_3$, it can be changed into a p-type material by substituting Fe to Ti ions [7]. Some previous work revealed the interesting properties such as ferroelectric [8], photochromic [9], oxygen sensitive properties [10, 11], as well as Jahn-Teller distortion. In addition, dielectric properties, defect state and conduction mechanism have been studied in strontium ferrate titanate system [12-15].

Last several years, strontium ferrate titanate has been attracted more and more attentions in studying defect chemistry, carrier transport properties and ferroelectric [16, 17]. Compared with the pure $SrTiO_3$, defect state like oxygen vacancies in strontium ferrate titanate sustains charge balance due to the diverse valence states between Fe and Ti ions. The formation of vacancies and defect state affects both electrical and magnetic behaviors [18]. As previous reports said, the potential barrier height is influenced as a result of oxygen vacancies concentration and chemisorption of O^- and O^{2-} at the grain boundary [19]. Fe ion doping of 10 % content improves the ferroelectric of $SrTiO_3$ exactly. Moreover, ferromagnetic properties in perovskites depend on not only oxygen vacancies and defects but also the annealing

atmosphere and temperature [20]. Afterwards, effects of annealing atmosphere on device performances were investigated [21, 22].

Up to present, iron-substituted $SrTiO_3$ system has been studied by multifarious experimental and theoretical researches. Nevertheless, there is still not any thorough elucidation of the relation to the concentration of point defects. An intensive understanding of the energy band regulation-property relation is essential. In this work, we presented the preparation and electric properties including resistive switching characteristic, ferroelectric and optoelectronic of $SrFe_{0.1}Ti_{0.9}O_{3-\sigma}$ thin film deposited on FTO/Glass substrate via chemical solution deposition method. In this article, it is the first time that electronic structure of $SrFe_xTi_{1-x}O_{3-\sigma}$ materials with different Fe ions doping content was studied via the first-principles method based on density functional theory to elaborate the experimental results.

2. Experimental

The method we used in our work to prepare the $SrFe_{0.1}Ti_{0.9}O_{3-\sigma}$ (abbreviated to SFTO) thin film on the FTO-coated glass substrate was chemical solution deposition. The raw materials we selected were strontium acetate, iron 9-hydrate nitrate and butyl titanate. In addition, methanol, 36% acetic acid and acetylacetone were selected as solvent and stabilizer respectively. First, strontium acetate was dissolved in methanol and iron nitrate was dissolved in 36% acetic acid. In order to dissolve the strontium acetate and iron 9-hydrate nitrate completely, we put the beaker on the heating table and stirred it for 2 hours to be dissolved at a temperature of 50°C. Secondly, appropriate amount of butyl titanate was taken from the measuring cylinder, and 2 drops of acetylacetone were added to stabilize it. Finally, we mixed the three solutions together and bottled the mixed solution after filtering. The concentration of the final mixed solution was 0.2 mol/L. In order to ensure the quality of the prepared thin film, we put the prepared solution stand at room temperature for one day and observed that there was no precipitate before casting the film. FTO-coated glass substrates were cleaned completely before the preparation. The solution was dropped onto the FTO substrate and spun at a speed of 4000 rpm for 30 seconds. Two high speed spins were performed according to the thickness of the required film. After that, thin film samples were baked on a heating table at 400°C for 30 min. We used the hydrofluoric acid to wipe one corner of the thin film samples in order to plate the electrode on the surface after annealing. At the end, the thin film samples were annealed at 650°C for 15 min in the oxygen atmosphere by the rapid thermal annealing furnace RTP-1000D4 facility.

X-ray diffraction, X-ray photoelectron spectroscopy and ERP were used to characterize the structure, chemical states and defect center of the thin film samples. The current-voltage (I-V) characteristic of the Au/SFTO/FTO/Glass device was measured with the two-probe method by the Keithley 2400 programmable electrometer under room temperature. Additionally, first principles calculations based on density functional theory were used to analyze the band structure and electronic states of the SFTO samples.

3. Results And Discussion

3.1. Structure, Morphology and Chemical States

To prove the crystalline state of the strontium ferrate titanate thin film we prepared, X-ray diffraction was applied to characterize the structure of the samples. Fig. 1 shows the X-ray diffraction result of the SFTO/FTO/Glass device. It can be seen from the periodic table of chemical elements, the ionic radius of iron is smaller than that of titanium. According to the Bragg diffraction equation, the XRD diffraction peaks of SFTO shift slightly too small angle. Peaks of (100), (110), (200) and (211) crystal planes of SFTO were observed, which indicates that SFTO thin film is crystallized in cubic structure. No second phase was observed in the X-ray diffraction result. Therefore, Fe ions successfully replace Ti ions in strontium titanate matrix and the same perovskite structure of strontium ferrite as strontium titanate is formed [23]. The SEM result of the section is shown in Figure 2(a). Figure 2(b) is the morphology observed by the atomic force microscope. As can be seen from the results of the image, the top layer is the strontium ferrate titanate thin film, while the middle layer is FTO conductive layer, and the bottom layer is glass. The thickness of the film is about 120 nm, and the particles are relatively dense [24].

In order to analyze the chemical composition, proportion and chemical valence of SFTO thin film sample, X-ray photoelectron spectroscopy (XPS) result is shown in Figure 3. Narrow spectrum scanning were acquired from the XPS spectra for the Sr 3d, Ti 2p, O 1s and Fe 2p levels of $SrFe_{0.1}Ti_{0.9}O_{3-\sigma}$ thin film sample. Two peaks of Sr 3d locate at 132.10 eV (Sr $3d_{5/2}$) and 133.78 eV (Sr $3d_{3/2}$) are observed in Fig. 3(a), which indicates Sr ions with chemical state of 2+ [25]. Two peaks of Ti $2p_{3/2}$ and Ti $2p_{1/2}$ are located at 457.52 eV and 463.24 eV in Fig. 3(b), which indicates Ti ions with chemical state of 4+. The O 1s spectra is shown in Figure 3(c) and the binding energy of O 1s spectra possess two peaks. The stronger peak appears at 528.59 eV and it is closely related to O^{2-} ions which is associated with O element in SFTO lattice [4]. The lower peak at 530.54 eV is owing to intermediate oxidation state for O element. It may be related to the chemical-adsorbed oxygen on the thin film surface, which is associated with defects such as oxygen vacancies. As shown in Fig. 3(d), Fe 2p XPS spectrum contains a doublet of Fe $2p_{3/2}$ and $2p_{1/2}$. The positions of the peaks are located at 709.60 eV and 723.25 eV, respectively. It indicates Fe element with chemical state of 3+ [26]. Due to spin-orbit coupling, Fe $2p_{3/2}$ peak is stronger than Fe $2p_{1/2}$ peak. In addition, the bimodal spectra of Fe 2p indicates Fe element with 4+ valence [27]. Therefore, both Fe^{3+} and Fe^{4+} ions exist in SFTO thin film [28]. It has been reported in the literature that the increase of charge at the Fe site leads to the shifting of Fe 2p spectrum toward higher binding energy [29]. Thus, it can be concluded that $SrTiO_3$ with 10% Fe ion doping can increase Fe^{3+} and Fe^{4+} ions effectively, resulting in the formation of oxygen vacancy defects.

3.2. Current-Voltage Characteristics

Resistive switching behavior of Au/SFTO/FTO/Glass device is shown in Figure 4. Voltage sweeping (0 → -3 → 0 → +3 → 0 V) is employed for I-V measurement. It can be seen from Figure 4b that the current of the Au/SFTO/FTO/Glass device increases with the gradual increase of negative voltage at the beginning,

and the device is in a low resistance state (LRS), as shown in path 1 in the Fig. 4(b). When the negative bias exceeds the threshold voltage of 2.8 V, the current rapidly decreases from 1.7×10^{-2} mA to 6×10^{-4} mA, and the state of the device switches from low resistance state (LRS) to high resistance state (HRS). As the negative bias decreases, the current approaches 0, as shown in path 2. When the scanning voltage is from 0 to 3 V, the current of the thin film device gradually increases from the zero. When the voltage exceeds the forward threshold voltage of 2.95 V, the current drops rapidly, and the device switches from low resistance state (LRS) to high resistance state (HRS), as shown in path 3. When the forward bias gradually decreases from 3 V to 0, the current intensity also decreases to zero, returning to the original state. At this point, a complete cycle test is completed. It can be concluded that the SFTO thin film device has the resistance switching behavior and the performance of memristors. Under the same test conditions, the resistive switching characteristics of $SrTiO_3$ cannot be found. We will discuss the reasons in the following sections. Figure 4c shows the I-V curve under semi-logarithmic coordinates. We can calculate the switch ratio from the figure 4(c). Switch ratio (R_{High}/R_{Low}) at -2.8 V is about 30. We also tested the switch retention characteristics to ensure the resistive switching stability of the strontium ferrate titanate. The results are shown in Figures 5(a) and (b). Resistances of HRS and LRS are read at -2.8 V and +2.8 V. Average ratio of HRS/LRS are about 30 and 10 respectively. From the results we can conclude that the resistive switching property of strontium ferrate titanate has not only good stability but also higher switching ratio compared with the pure strontium titanate.

In order to figure out the resistive switching mechanism of Au/SFTO/FTO/Glass device, I-V characteristics under negative and positive applied bias are replotted as Log I vs. Log V and shown in Figure 6a,b respectively. The slopes of fitting curve in LRS under negative and positive applied bias are 1.05 and 1.09, corresponding to Ohmic conduction mechanism. For HRS, Ohmic conduction mechanism is dominant in low voltage region under both negative and positive applied bias, which is confirmed by the slopes of fitting curves of 1.05 and 1.07. However, conduction mechanism switches to space-charge limited current (SCLC) mechanism in high voltage region, which is confirmed by the slopes of fitting curves of 1.93 and 2.13. In general, SCLC mechanism is mainly related the presence of defect centers. The current density of space-charge limited current can be explained as follow:

$$J_{SCLC} = \frac{9V^2}{8d^3}\varepsilon\mu \qquad (1)$$

Where V is the bias voltage, d is the thickness of the thin film, ε is the dielectric constant of the thin film and μ is the electron mobility. Under the application of bias voltage, the defect centers can capture the free carriers excited by the electric field. In order to understand the conduction mechanism of strontium ferrate titanate thin film devices more intuitively, a reasonable model is proposed to explain the role of oxygen vacancy in the conduction process which is shown in Figure 7.

Oxygen vacancies are inevitable in the preparation of thin films and the redistribution of electric charge on the surface of the devices is generated when the electrodes are plated to form the structure of the

strontium ferrate titanate thin film devices. Therefore, before the device structure is formed without bias voltage, due to different work functions of the metal electrode and the strontium ferrate titanate thin film, the two different materials contact at the interface and form the Schottky junction. The electrons cannot freely cross the Schottky barrier, and the Fermi level of the gold electrode is at the same level with the Fermi level of the strontium ferrate titanate thin film which is shown in Figure 7a. When the forward bias voltage is added, the potential barrier at the interface will decrease, the Fermi energy level of the strontium ferrate titanate thin film will rise, and the electrons will fill into the oxygen vacancy and be captured by the oxygen vacancy. A large number of electrons tend to move towards the direction of the gold electrode, forming a low resistance state (LRS), as shown in Figure 7b. When the reverse bias voltage is applied, the barrier at the interface will increase, the oxygen vacancy will release the captured electrons, and the Fermi energy level of the film will decrease. However, due to the increase of the barrier, only a small part of the electrons on the surface of the gold electrode can cross the barrier and enter the conduction band of the semiconductor thin film, thus forming a high resistance state (HRS) which is shown in Figure 7c. When the direction of electric field is constantly changed, the strontium ferrate titanate thin film device can switch between high and low resistance states. Additionally, the more oxygen vacancies the thin film has, the higher ratio of high and low resistance states the thin film would have. By doping Fe ions, the defect concentration of strontium ferrate titanate thin film can be changed to produce more oxygen vacancies which affect the migration of the free electrons. Thus, by contrasting the I-V characteristics between the strontium ferrate titanate thin film and the pure strontium titanate thin film (Figures 4(b) and 4(c)) and the conduction mechanism simulation diagram analysis (Figure 7), we can draw the conclusion that strontium ferrate titanate thin film has relatively favorable resistive switching performance due to the increase of oxygen vacancies.

3.3. Optical Properties

The UV-visible absorption spectrum of the SFTO thin film is shown in Figure 8a. SFTO thin film absorbs more UV light with a wavelength lower than 365 nm, and the UV response is relatively sensitive. According to Tauc's law, the relationship between absorption coefficient and photon energy can be expressed as:

$$E=hC/\lambda, \quad (2)$$

The optical band gap (E_g) can be derived by the tangent line of the known curve. E_g of 2.84 eV is obtained for SFTO thin film as shown in Figure 8b, being lower than the E_g of pure $SrTiO_3$ (3.24 eV). The doping of Fe ions can lower the E_g of strontium titanate. Thus, SFTO thin films have better electric properties.

In order to determine the defect type of the thin film of strontium titanate with 10% Fe irons doping, we studied its electron paramagnetic resonance (EPR) spectra. EPR is a magnetic resonance technique used

to characterize the unpaired electrons or single electron states of materials. From the EPR spectra, g factor of the sample can be calculated and used to determine whether there is an electron defect center or a whole defect center by comparing it with the g factor of the free electron. Some researchers used EPR technology to analyze O^{2-} ions and Ti^{3+} ions on the surface of polycrystalline TiO_2 and $SrTiO_3$, respectively [30, 31]. Figure 9 shows the EPR result of SFTO thin film sample. It is find that the EPR peak occurs at a position of 3800 gauss magnetic field intensity. The *g* factor of strontium titanate SFTO thin film sample can be calculated by the following formula:

$$g = 0.7144773 \times v/B_0 , \quad (3)$$

Where *n* is frequency and B_0 is magnetic field. *g* factor of SFTO thin film sample is 1.9237, which is less than that of free electron (2.0023), indicating that there is an electron defect center in thin film sample. To some extent, it can be concluded that Fe ions have successfully replaced the Ti ions in strontium titanate matrix. Fe ions can attract more electron density distribution than Ti ions and lead to the redistribution of electron cloud density near the Fe-doped impurity, which is closely related to the formation of oxygen vacancies. .

3.4. First-Principles Calculations

It has been reported that a phenomenon of Jahn-Teller distortion in strontium ferrate titanate was found [16]. It is closely related to the Fe-O bond length. Fe-O bond length will change when Fe ions substitute to Ti ions, producing relative displacement of oxygen and related oxygen defects. Experiments show that Jahe-Teller distortion decreases with the increase of Fe ions concentration. Further analysis on electronic state density, band structure and absorption spectrum is studied via first principles calculation based on density functional theory for SFTO. In order to better illustrate the band structure and electron state density of $SrFe_{0.1}Ti_{0.9}O_{3-\sigma}$, $SrTiO_{3-\sigma}$ and $SrFeO_{3-\sigma}$ are also studied. Calculation results are shown in the Figure 10. Among them, Figures 10(a) and 10(b) shows the band structure and electron state density of $SrTiO_{3-\sigma}$. The top of the valance band and the bottom of conduction band are mainly made up of O 2p states and Ti 3d states, respectively. Figures 10(e) and 10(f) illustrate the band structure and electron state density of $SrFeO_{3-d}$. It is obviously seen from the comparison of the electron state density for spinning up and spinning down of the electron densities, where the effect of spin polarization is derived from the Fe 2p states, a little bit from Fe 3d states. The results in Figure 10e,f also indicate that there is a strong superposition of Fe 3d orbital electron states and O 2p orbital electron states near the Fermi level. In addition, the contribution of the main electron states near the Fermi level is derived from the Eg states of the Fe ions and O 2p electron states. Figures 10(c) and 10(d) show the band structure and electron state density of $SrFe_{0.1}Ti_{0.9}O_{3-\sigma}$. The top of the valence band consists of O 2p orbital electron states, while the bottom of virtual bands mainly originates from Ti 3d electron states. It can be concluded that the band gap of strontium titanate with 10% Fe-doping is smaller than that of pure strontium titanate,

which indicates that Fe ions can regulate the energy band of strontium titanate and form the defect state effectively.

4. Conclusions

In the paper, the resistance characteristics and band structure of strontium ferrate titanate /FTO devices are studied. Polycrystalline strontium ferrate titanate thin films were successfully prepared on FTO/Glass substrate by chemical solution deposition. XRD results showed that the characteristic peaks of strontium ferrite titanate were consistent with that of polycrystalline strontium titanate. It can be seen from SEM that the grains of strontium ferrate titanate films are relatively dense and have good crystallinity. The analysis results of EPR and XPS show that Fe ions can produce oxygen vacancy and other defects, and form electron trap center, which has important influence on the resistance characteristics of strontium ferrate titanate. Typical bipolar resistance is easy to be found in the test. By means of log-log fitting, we found that Ohmic conduction is the conduction mechanism in the low resistance state, and Ohmic conduction and space charge limited current conduction are the two mechanisms in the high resistance state. The first principles calculation shows that the band structure of strontium titanate has changed after the doping of Fe ions. In addition, through the absorption spectrum test of strontium ferrate titanate, it was found that the absorption of partial visible light was enhanced. By absorption spectrum calculation, the band gap width Eg of the sample was 2.84 eV, slightly smaller than the band gap width 3.24 eV of strontium titanate. The experimental results were consistent with the theoretical calculation.

5. Declarations

Acknowledgments

This work was supported by the National Natural Science Foundation of China (Grant No. 11574057), and the Science and Technology Program of Guangdong Province of China (Grant No. 2017A010104022).

6. References

[1] Cho S, Jang JW, Zhang W, et al. MacManus-Driscoll, J.L. Single-crystalline thin films for studying intrinsic properties of $BiFeO_3$–$SrTiO_3$ solid solution photoelectrodes in solar energy conversion. *Chem. Mate*r. **2015**, *27*, 6635-6641.

[2] Janousch M, Meijer GI., Staub U, et al. Role of oxygen vacancies in Cr-doped $SrTiO_3$ for resistance-change memory. *Adv. Mater.* 2007, *19*, 2232-2235.

[3] Menesklou W, Schreiner HJ, Hardtl KH. High temperature oxygen sensors based on doped $SrTiO_3$. *Sensor Actuat. B-Chem*. **1999**, *59*, 184-189.

[4] Kawasaki S, Nakatsuji K, Yoshinobu J, et al. Epitaxial Rh-doped $SrTiO_3$ thin film photocathode for water splitting under visible light irradiation. *Appl. Phys. Lett*. **2012**, *101*, 033910.

[5] Wang L, Merkle R, Mastrikov YA, et al. Oxygen exchange kinetics on solid oxide fuel cell cathode materials—general trends and their mechanistic interpretation. *J. Mater. Res*. **2012**, *27*, 2000-2008.

[6] Alexandrov VE, Maier J, Evarestov RA. Ab initio study of $SrFe_xTi_{1-x}O_3$: Jahn-Teller distortion and electronic structure. *Phys. Rev. B*. **2008**, *77*, 075111.

[7] Higuchi T, Tsukamoto T, Sata N, et al. Electronic structure of p-type $SrTiO_3$ by photoemission spectroscopy. *Phys. Rev. B* **1998**, *57*, 6978.

[8] Sarin N, Mishra M, Gupta G, et al. Deciphering the Role of Oxygen Vacancies on Structural, Electrical, and Magnetic Properties of Fe-Substituted Strontium Titanate. *Phys. Status Solidi B*. **2018**, *255*, 1700683.

[9] Berney RL, Cowan DL. Photochromism of three photosensitive Fe centers in SrTiO3. Phys. Rev. B 1981, 23, 37.

[10] Merkle R, Maier J. Oxygen incorporation into Fe-doped $SrTiO_3$: Mechanistic interpretation of the surface reaction. *Phys. Chem. Chem. Phys*. **2002**, *4*, 4140-4148.

[11] Rothschild A, Litzelman SJ, Tuller HL, et al. Temperature-independent resistive oxygen sensors based on $SrTi_{1-x}Fe_xO_{3-\delta}$ solid solutions. *Sensor Actuat. B-Chem.* **2005**, *108*, 223-230.

[12] Ang C, Yu Z, Jing Z, et al. Dielectric spectra and electrical conduction in Fe-doped $SrTiO_3$. *Phys. Rev. B* **2000**, *61*, 3922.

[13] Hao L, Xue Q, Gao X, et al. Abnormal I-V characteristics and metal-insulator transition of Fe-doped amorphous carbon/silicon p-n junction. *J. Appl. Geophys*. **2007**, *101*, 053718.

[14] Rothschild A, Menesklou W, Tuller HL. Electronic structure, defect chemistry, and transport properties of $SrTi_{1-x}Fe_xO_{3-y}$ solid solutions. *Chem. Mater*. **2006**, *18*, 3651-3659.

[15] Steinsvik S, Bugge R, Gjnnes J, et al. The defect structure of $SrTi_{1-x}Fe_xO_{3-y}$ (x= 0-0.8) investigated by electrical conductivity measurements and electron energy loss spectroscopy (EELS). *J. Phys. Chem. Solids*. **1997**, *58*, 969-976.

[16] Vracar M, Kuzmin A, Merkle R, et al. Jahn-Teller distortion around Fe4+ in $Sr(Fe_xTi_{1-x})O_{3-\delta}$ from X-ray absorption spectroscopy, X-ray diffraction, and vibrational spectroscopy. *Phys. Rev. B* **2007**, *76*, 174107.

[17] Rodewald S, Fleig J, Maier J. Microcontact impedance spectroscopy at single grain boundaries in Fe-doped $SrTiO_3$ polycrystals. *J. Am. Ceram. Soc*. **2001**, *84*, 521-530.

[18] Sundell PG, Bjorketun ME, Wahnstrom G. Thermodynamics of doping and vacancy formation in $BaZrO_3$ perovskite oxide from density functional calculations. *Phys. Rev. B* **2006**, *73*, 104112.

[19] Johnson KD, Dravid VP. Static and dynamic electron holography of electrically active grain boundaries in $SrTiO_3$. *Interface Sci.* **2000**, *8*, 189-198.

[20] Wang YG, Tang XG, Liu QX, et al. Ferroelectric and ferromagnetic properties of $SrTi_{0.9}Fe_{0.1}O_{3-\delta}$ thin films, *Solid State Commun*. **2015**, *202*, 24-27.

[21] Baker JN, Bowes PC, Long DM, et al. Defect mechanisms of coloration in Fe-doped $SrTiO_3$ from first principles. *Appl. Phys. Lett*. **2017**, *110*, 122903.

[22] Neaton JB, Ederer C, Waghmare UV, et al. First-principles study of spontaneous polarization in multiferroic $BiFeO_3$. *Phys. Rev. B* **2005**, *71*, 014113.

[23] Carter E, Carley AF, Murphy DM. Evidence for O_2-radical stabilization at surface oxygen vacancies on polycrystalline TiO_2. *J. Phys. Chem. C* **2007**, *111*, 10630-10638.

[24] Caretti I, Van D, Sabine, et al. Light-induced processes in plasmonic gold/TiO_2 photocatalysts studied by electron paramagnetic resonance. *Top. Catal.* **2015**, *58*, 776-782.

[25] Huang MH, Xia JY, Xi YM, et al. Study on photochromism in $SrTiO_3$: Fe ceramic powder. *J. Eur. Ceram. Soc*. **1997**, *17*, 1761-1765.

[26] Ehre D, Cohen H, Lyahovitskaya V, et al. X-ray photoelectron spectroscopy of amorphous and quasiamorphous phases of $BaTiO_3$ and $SrTiO_3$. *Phys. Rev. B* **2008**, *77*, 184106.

[27] Fuentes S, Munoz P, Barraza N, et al. Structural characterisation of slightly Fe-doped $SrTiO_3$ grown via a sol-gel hydrothermal synthesis. *J. Sol-Gel Sci. Tech*. **2015**, *75*, 593-601.

[28] Merino NA, Barbero BP, Eloy P, et al. $La_{1-x}Ca_xCoO_3$ perovskite-type oxides: identification of the surface oxygen species by XPS. *Appl. Surf. Sci.* **2006**, *253*, 1489-1493.

[29] Ghaffari M, Liu T, Huang H, et al. Investigation of local structure effect and X-ray absorption characteristics (EXAFS) of Fe (Ti) K-edge on photocatalyst properties of $SrTi_{(1-x)}Fe_{(x)}O_{(3-\delta)}$. *Mater. Chem. Phys*. **2012**, *136*, 347-357.

[30] Ghaffari M, Shannon M, Hui H, et al. Irannejad, A. Preparation, surface state and band structure studies of $SrTi_{(1-x)}Fe_{(x)}O_{(3-\delta)}$(x= 0-1) perovskite-type nano structure by X-ray and ultraviolet photoelectron spectroscopy. *Surf. Sci*. **2012**, *606*, 670-677.

[31] Sahner K, Schonauer D, Moos R, et al. Effect of electrodes and zeolite cover layer on hydrocarbon sensing with p-type perovskite $SrTi_{0.8}Fe_{0.2}O_{3-\delta}$ thick and thin films. *J. Mater. Sci.* **2006**, *41*, 5828-5835.

[32] Bocquet AE, Fujimori A, Mizokawa T, et al. Electronic structure of $SrFe^{4+}O_3$ and related Fe perovskite oxides. *Phys. Rev. B* **1992**, *45*, 1561.

[33] Du H, Jia CL, Mayer J, et al. Atomic Structure of Antiphase Nanodomains in Fe-Doped $SrTiO_3$ Films. *Adv. Funct. Mater.* **2015**, *25*, 6369-6373.

Figures

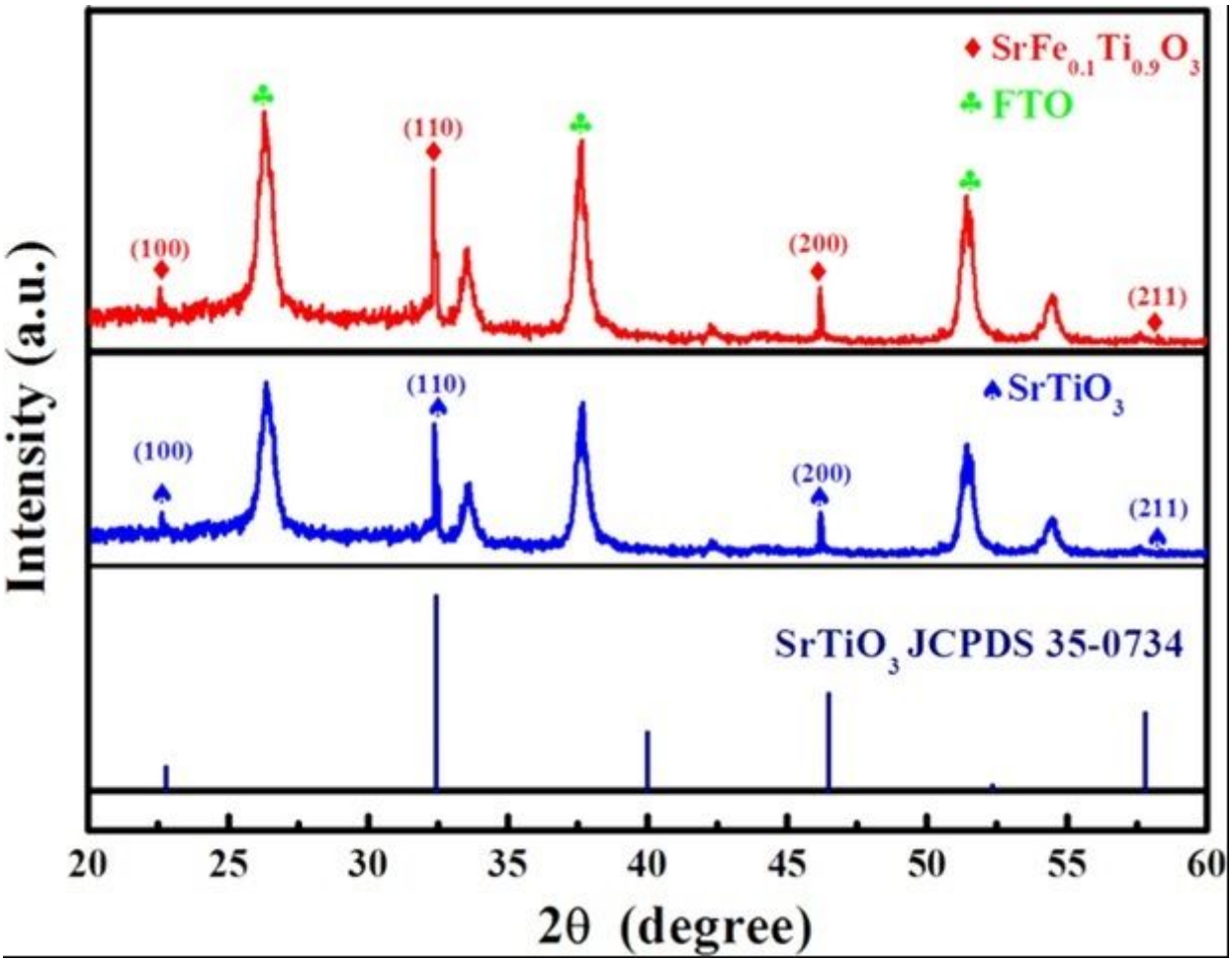

Figure 1

The XRD patterns of the SFTO film on FTO/Glass substrates.

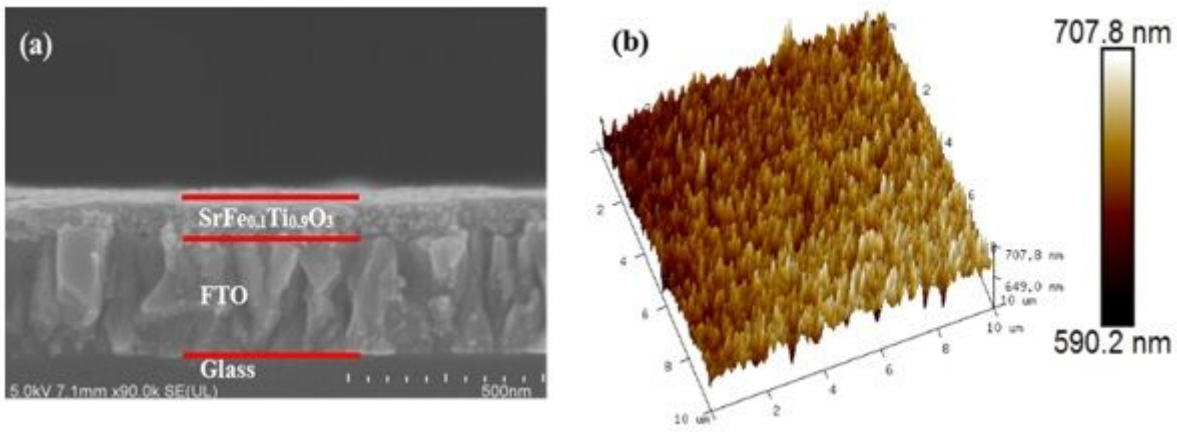

Figure 2

(a) Cross section SEM image and (b) AFM image of the SFTO/FTO/Glass device.

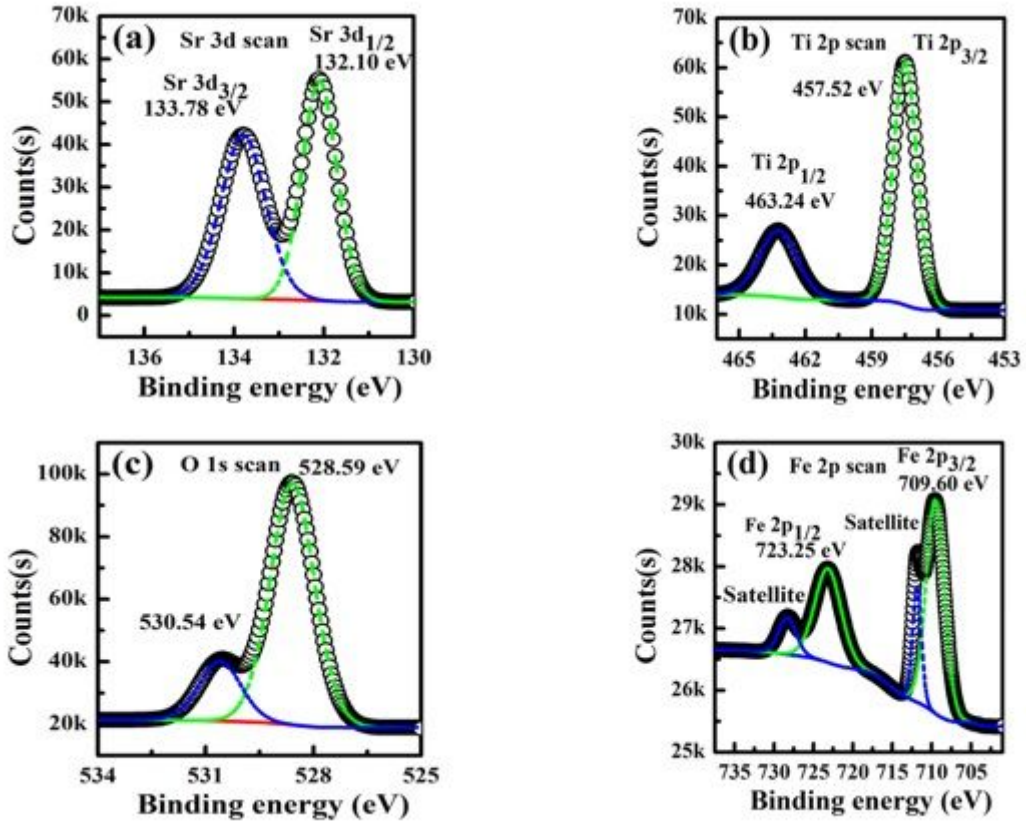

Figure 3

XPS survey of the SrFe0.1Ti0.9O3-σ thin film and the fitted narrow sweeping results of (a) Sr 3d, (b) Ti 2p, (c) O 1s, and (d) Fe 2p.

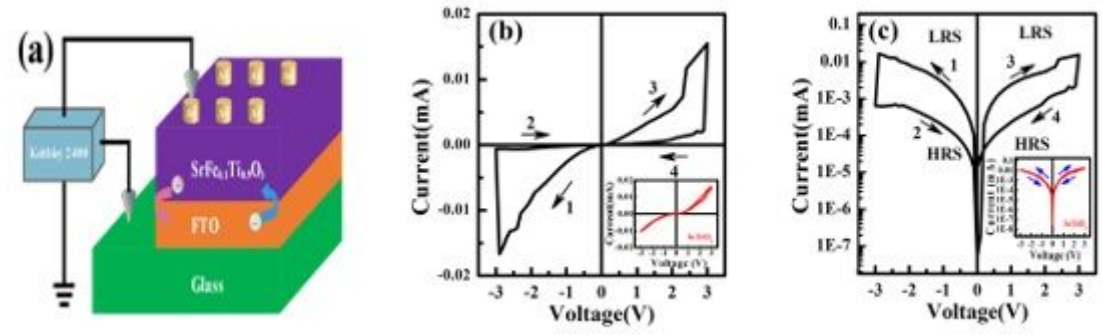

Figure 4

Resistance properties of the SFTO/FTO/Glass device. (a) Measurement schematic diagram of the Au/SFTO/FTO/Glass device. (b) I-V characteristic curve in Cartesian coordinates at the bias voltage of ±3V and I-V characteristics measuring structure is shown in the illustration as well. The illustration is the I-V characteristic of pure SrTiO3 in Cartesian coordinates. (c) I-V characteristic curve in logarithmic coordinates and the direction of measurement is shown in the order of arrows from 1 to 4. The illustration is the I-V characteristic of pure SrTiO3 in logarithmic coordinates.

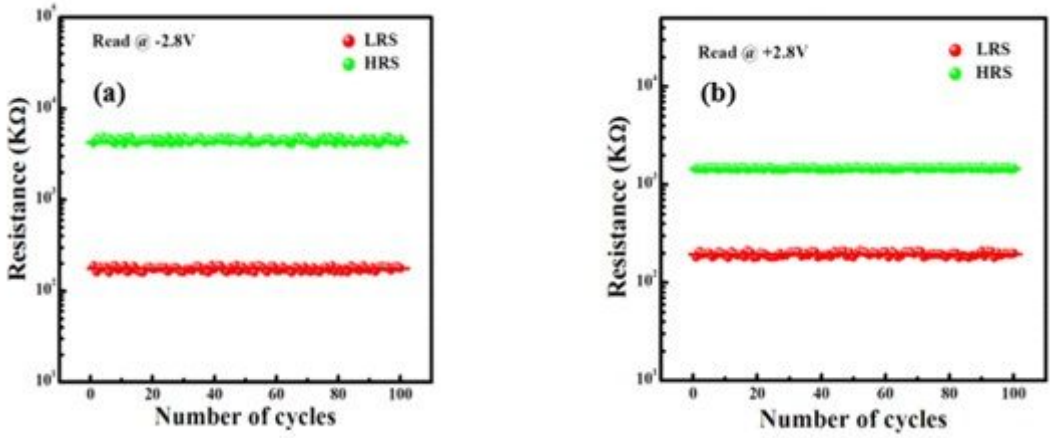

Figure 5

Resistance retention characteristics of the SFTO/FTO/Glass device

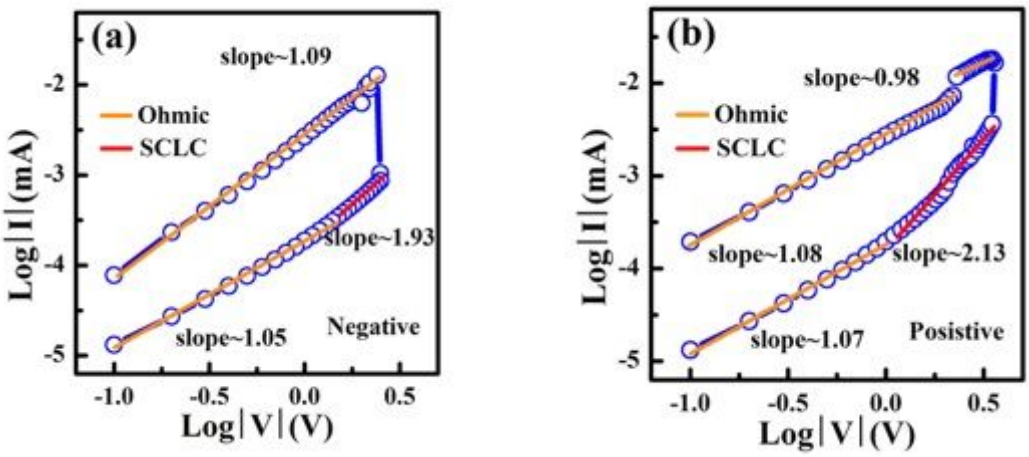

Figure 6

Analysis of the conductance mechanism under negative (a) and positive (b) voltage bias fitted by double logarithm, respectively.

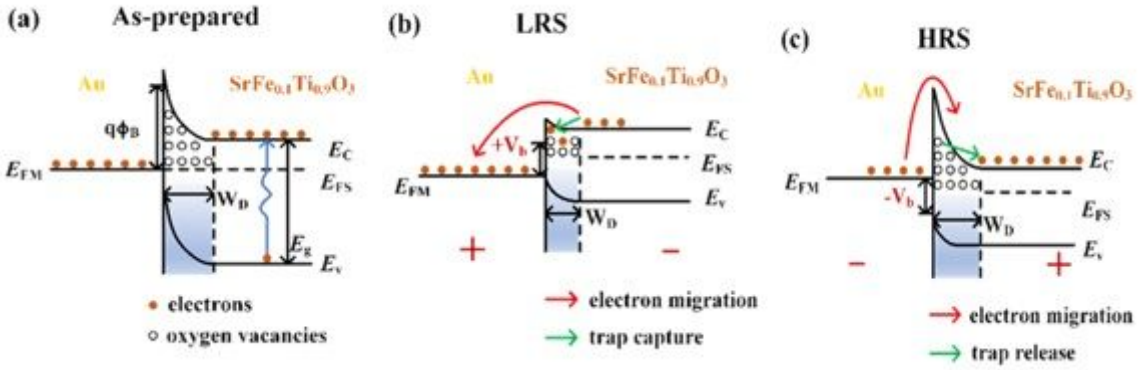

Figure 7

The schematic diagram of the resistance switching phenomenon of SFTO/FTO/Glass device based on the Schottky barrier.

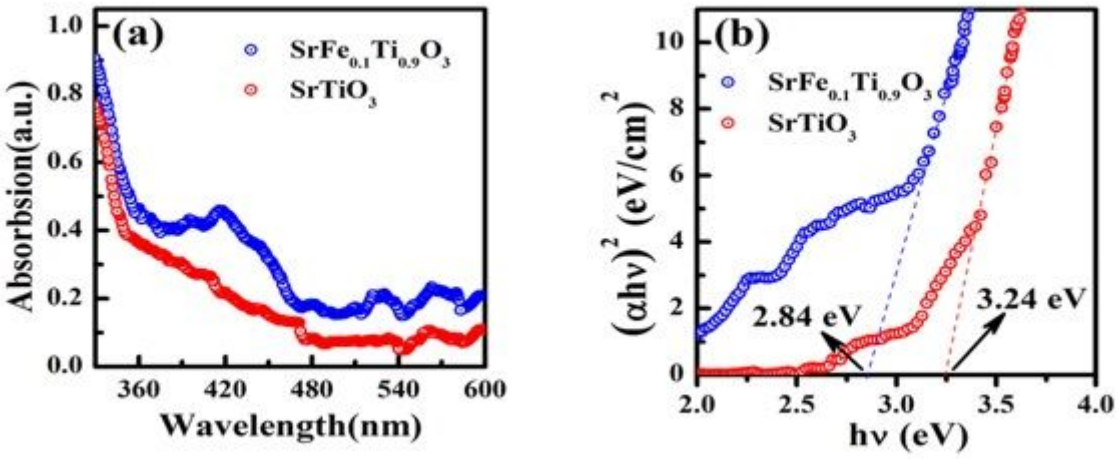

Figure 8

Comparison of optical properties between Fe doped strontium titanate and pure strontium titanate. (a)UV-visible absorption spectrum with the wavelength range from 330 nm to 600 nm. (b) The calculated band gap results are the points at which the tangent line intersects the horizontal axis according to the Tauc's law.

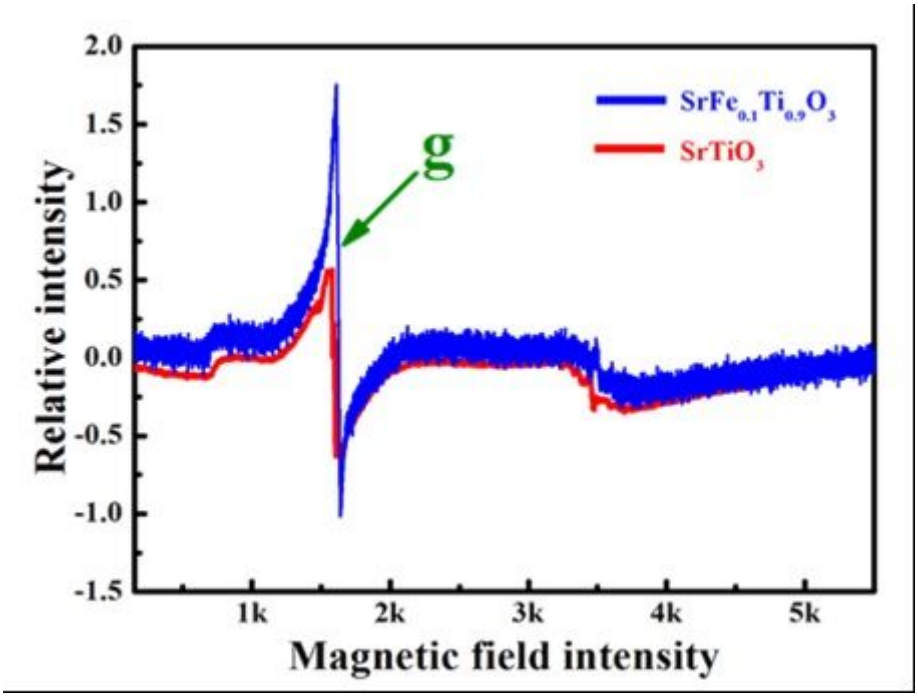

Figure 9

Electron paramagnetic resonance (EPR) spectroscopy of strontium titanate films with iron content of 10%. The defect type can be determined by calculating g from the figure.

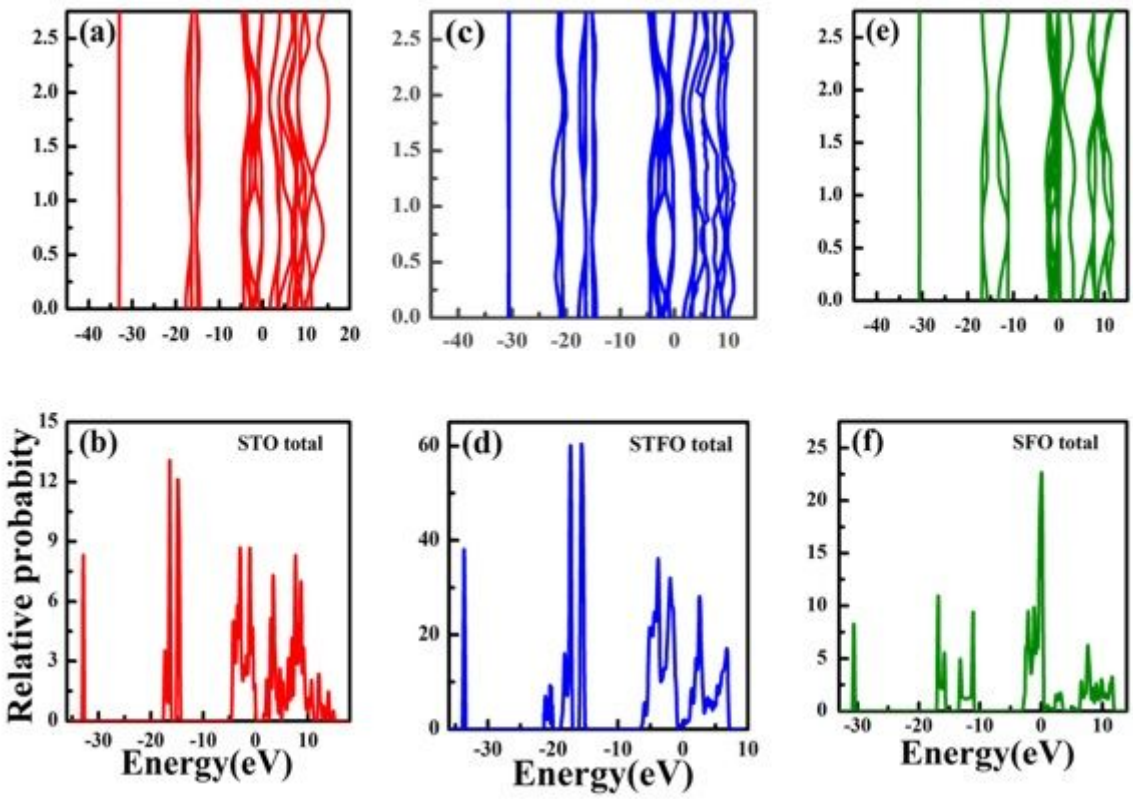

Figure 10

Calculated band structures and density of electron states for (a) and (b) SrTiO3, (c) and (d) SrFe0.1Ti0.9O3-σ, (e) and (f) SrFeO3. In all cases the presentation of the valence band and conduction band are concluded.